Supplemental material.

Supplemental figure 1. TLR2/GFP correlation in immunostaining. H&E staining of dorsal skin of WT mice. TLR2 dynamic during the second telogen.

Supplemental figure 2. Confocal images of hair follicles immunostained for P-cad

Supplemental figure 3. Bulge stem cell marker expression in TLR2$^{\text{HFSC-KO}}$ mouse.

Supplemental figure 4. TLR2-BMP axis in hair follicle cells. BMP signaling in the hair bulge of WT and TLR2$^{\text{HFSC-KO}}$ mice.

Supplemental figure 5. MPO expression in sebaceous gland of hair follicles from old vs young mice; effect of CEP in-vitro and in-vivo on hair follicle growth.

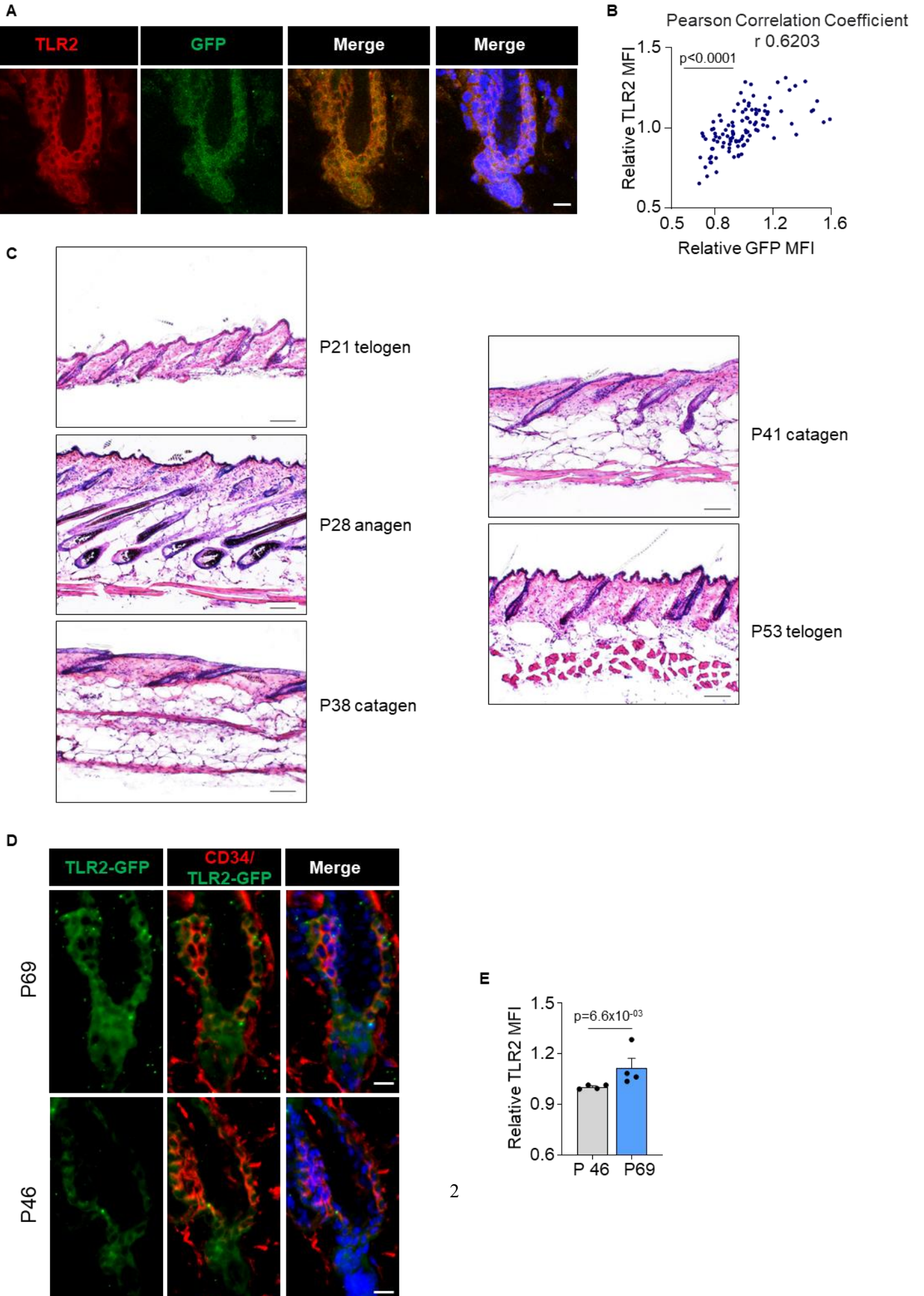**Supplemental table 1.** qPCR primers.

Supplementary figure 1

A

| TLR2 | GFP | Merge | Merge |

B

Pearson Correlation Coefficient
r 0.6203

p<0.0001

Relative TLR2 MFI

Relative GFP MFI

C

P21 telogen

P28 anagen

P38 catagen

P41 catagen

P53 telogen

D

| TLR2-GFP | CD34/ TLR2-GFP | Merge |

P69

P46

E

p=6.6x10^{-03}

Relative TLR2 MFI

P 46   P69

2

Fig. S1.

A. Confocal images of dorsal skin hair follicles co-immunostained for TLR2 and GFP. Scale bars are 10 μm.

B. A scatter graph shows a high level of correlation between TLR2 and GFP intensity. N=3.

C. Representative H&E staining of the dorsal skin of WT mice at indicated time points demonstrates the typical changes in hair follicle morphology. Scale bars are 100 μm.

D. Confocal images of dorsal skin hair follicles from p46 and p69 mice immunostained for TLR2.

E. Bar graph showing an elevated level of TLR2 in HFSC of p69 mice (late second telogen) compared to p46 (early second telogen). N = 4

Correlation analysis and the Mann-Whitney test were used to determine the statistical significance. All data are mean ± s.e.m.
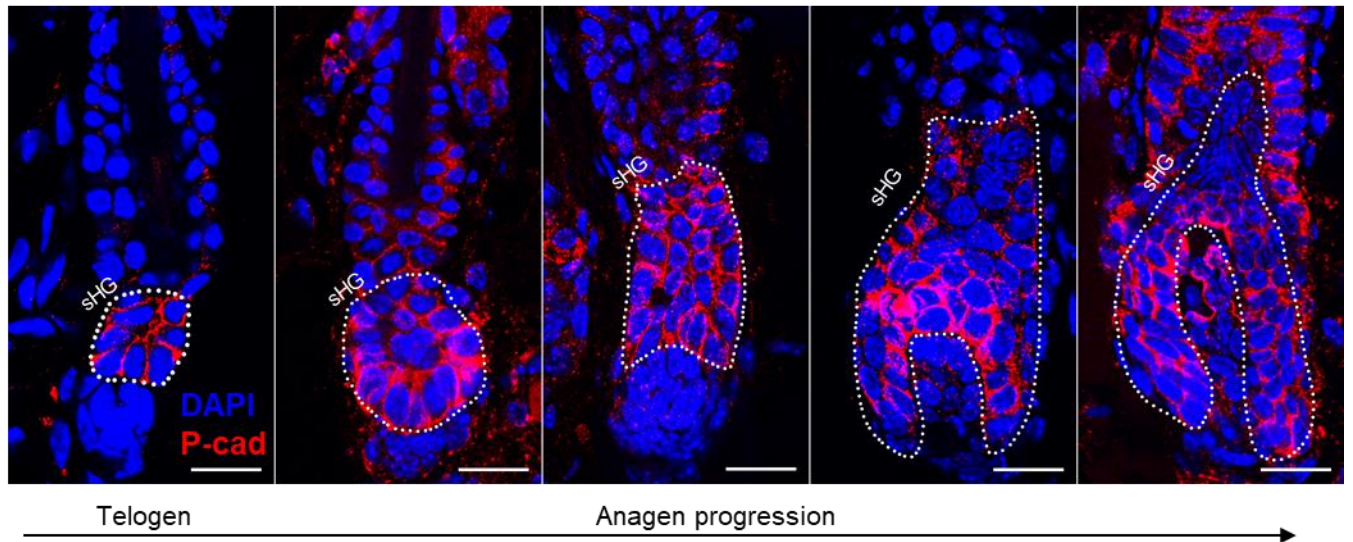
Supplementary figure 2

Telogen — Anagen progression

Fig.S2.

sHG enlargement and elongation at anagen onset.

Representative confocal images of hair follicles immunostained for P-cad showing changes in the size of sHG during the progression of the hair cycle. At anagen onset, sHG cells proliferate and grow downward to envelop the dermal papilla. The proliferation of sHG cells results in a larger sHG compared to telogen. Dashed lines outline the sHG. Scale bars are 20 μm.
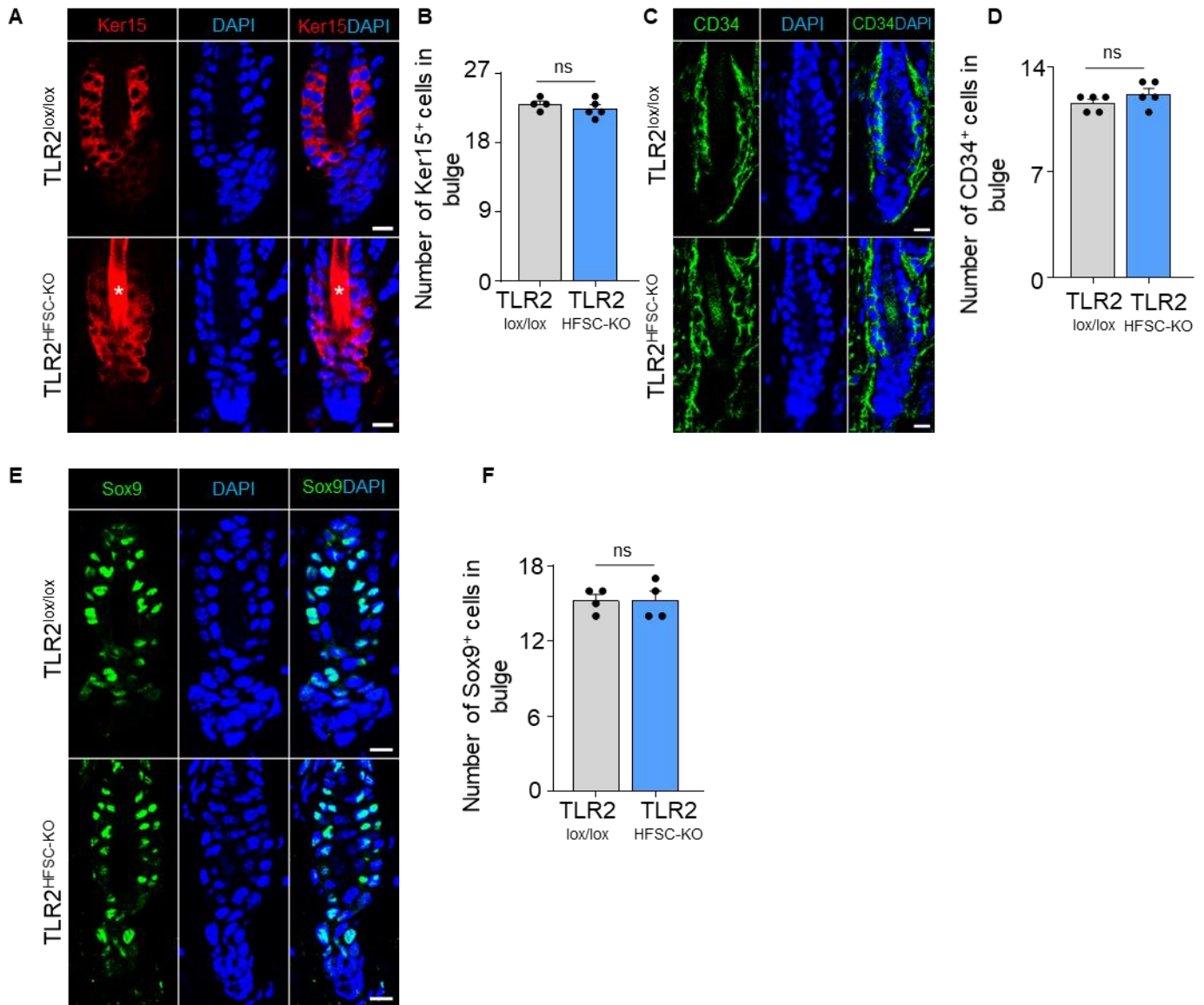
Supplementary figure 3

A

B

C

D

E

F

Fig.S3.

Bulge stem cell marker expression in TLR2$^{\text{HFSC-KO}}$ mouse.

A. Representative confocal images of telogen hair follicles from TLR2$^{\text{lox/lox}}$ and TLR2$^{\text{HFSC-KO}}$ mice immunostained for Ker15. Stars label the hair shaft. Scale bars are 10 μm.

B. Bar graph showing no difference in numbers of Ker15$^+$ cells in bulge area in TLR2$^{\text{lox/lox}}$ compared with TLR2$^{\text{HFSC-KO}}$ telogen hair follicles from images in A. N = 4 and 5 mice for TLR2$^{\text{lox/lox}}$ and TLR2$^{\text{HFSC-KO}}$ respectively.

C. Telogen hair follicles from TLR2$^{\text{lox/lox}}$ and TLR2$^{\text{HFSC-KO}}$ mice immunostained for CD34. Scale bars are 10 μm.

D. Quantification of CD34$^+$ cell numbers in bulge area in images from C showing no difference in TLR2$^{\text{lox/lox}}$ compared with TLR2$^{\text{HFSC-KO}}$ follicles. N = 5 per group.

E. Representative confocal images of TLR2$^{\text{lox/lox}}$ and TLR2$^{\text{HFSC-KO}}$ telogen hair follicles immunostained for Sox9. Scale bars are 10 μm.

F. Bar graph showing no difference in Sox9$^+$ cell numbers in bulge area in TLR2$^{\text{lox/lox}}$ and TLR2$^{\text{HFSC-KO}}$ follicles from images in E. N = 4.

Mann-Whitney test was used to determine the statistical significance. All data are mean ± s.e.m.
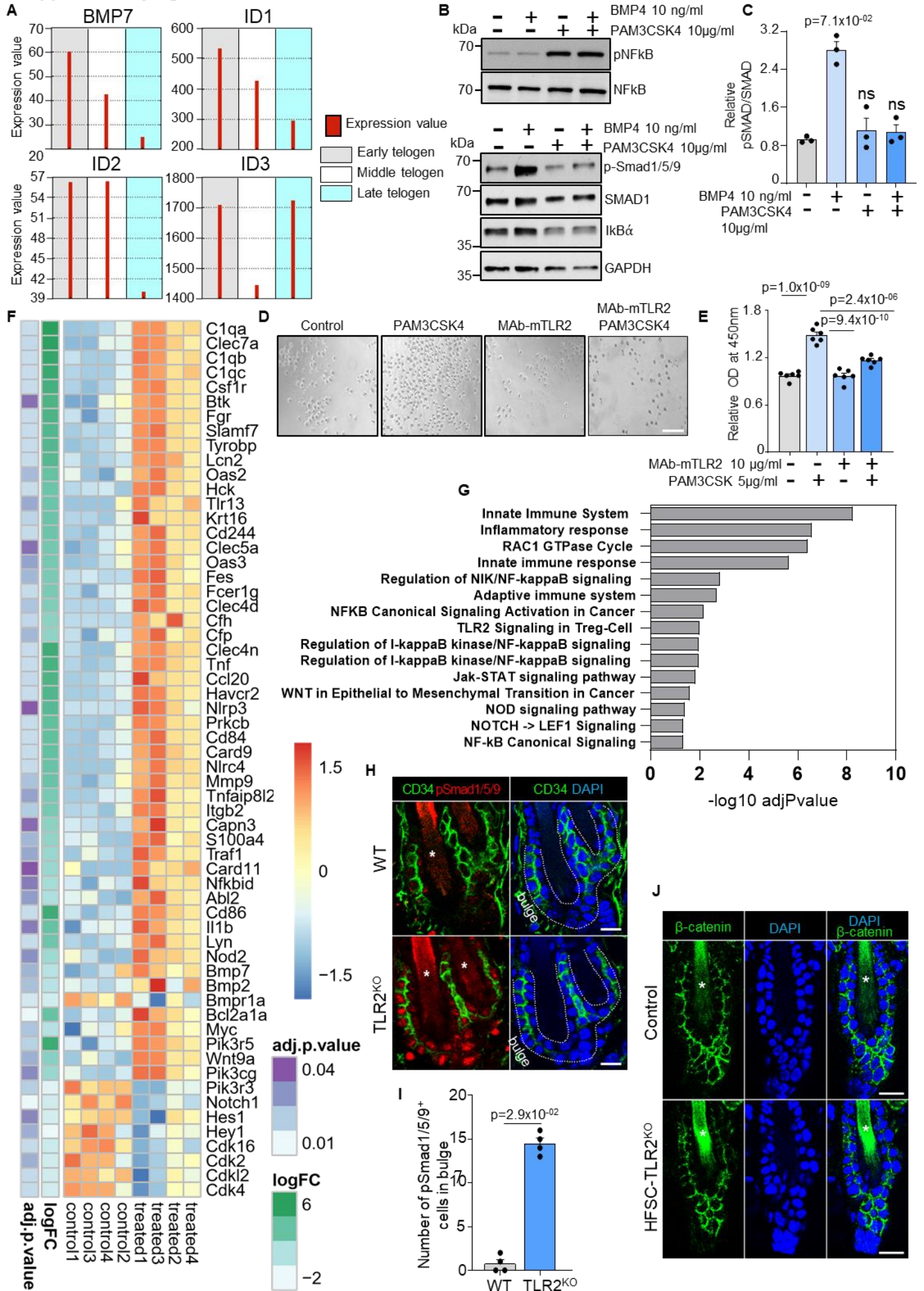
Supplementary figure 4

A

BMP7

Expression value (20–70)

ID1

Expression value (200–600)

ID2

Expression value (39–57)

ID3

Expression value (1400–1800)

- Expression value (red)
- Early telogen (grey)
- Middle telogen (white)
- Late telogen (cyan)

B

BMP4 10 ng/ml: − + − +
PAM3CSK4 10µg/ml: − − + +

kDa
70 — pNFkB
70 — NFkB

BMP4 10 ng/ml: − + − +
PAM3CSK4 10µg/ml: − − + +

kDa
70 — p-Smad1/5/9
70 — SMAD1
35 — IkBα
35 — GAPDH

C

Relative pSMAD/SMAD (0.8–3.2)

p=7.1x10^{-02}

ns   ns

BMP4 10 ng/ml: − + − +
PAM3CSK4 10µg/ml: − − + +

D

Control   PAM3CSK4   MAb-mTLR2   MAb-mTLR2 PAM3CSK4

E

Relative OD at 450nm (0–1.8)

p=1.0x10^{-09}
p=2.4x10^{-06}
p=9.4x10^{-10}

MAb-mTLR2 10 µg/ml: − − + +
PAM3CSK 5µg/ml: − + − +

F

C1qa, Clec7a, C1qb, C1qc, Csf1r, Btk, Fgr, Slamf7, Tyrobp, Lcn2, Oas2, Hck, Tlr13, Krt16, Cd244, Clec5a, Oas3, Fes, Fcer1g, Clec4d, Cfh, Cfp, Clec4n, Tnf, Ccl20, Havcr2, Nlrp3, Prkcb, Cd84, Card9, Nlrc4, Mmp9, Tnfaip8l2, Itgb2, Capn3, S100a4, Traf1, Card11, Nfkbid, Abl2, Cd86, Il1b, Lyn, Nod2, Bmp7, Bmp2, Bmpr1a, Bcl2a1a, Myc, Pik3r5, Wnt9a, Pik3cg, Pik3r3, Notch1, Hes1, Hey1, Cdk16, Cdk2, Cdkl2, Cdk4

Columns: adj.p.value, logFC, control1, control3, control4, control2, treated1, treated3, treated2, treated4

logFC scale: −1.5 to 1.5

adj.p.value: 0.04, 0.01
logFC: 6, −2

G

- Innate Immune System
- Inflammatory response
- RAC1 GTPase Cycle
- Innate immune response
- Regulation of NIK/NF-kappaB signaling
- Adaptive immune system
- NFKB Canonical Signaling Activation in Cancer
- TLR2 Signaling in Treg-Cell
- Regulation of I-kappaB kinase/NF-kappaB signaling
- Regulation of I-kappaB kinase/NF-kappaB signaling
- Jak-STAT signaling pathway
- WNT in Epithelial to Mesenchymal Transition in Cancer
- NOD signaling pathway
- NOTCH -> LEF1 Signaling
- NF-kB Canonical Signaling

-log10 adjPvalue (0–10)

H

CD34 pSmad1/5/9   CD34 DAPI

WT

TLR2^{KO}

bulge

I

Number of pSmad1/5/9$^+$ cells in bulge (0–20)

p=2.9x10^{-02}

WT   TLR2^{KO}

J

β-catenin   DAPI   DAPI β-catenin

Control

HFSC-TLR2^{KO}

Fig. S4.

A. GEO2R analysis of published RNA data from sorted follicle populations in the 2nd telogen to anagen transition demonstrates the declined expression of BMP7 mRNA and key transcriptional target of the BMP signaling pathway in the skin, ID1, ID2, and ID3 mRNA.

B. Western blot analysis of pNFkB, NFkB, pSMAD1/5/9, SMAD1, ikBα protein level in Human Epidermal Keratinocytes treated with/without 10 µg/ml Pam3SCK4 and 10 ng/ml BMP4.

C. Bar graphs show the activation effect of BMP4 treatment on the BMP signaling which was abolished in the presents of TLR2 ligand Pam3SCK4. N=3 independent experiments.

D. Representative microphotographs of Human Hair Follicle Stem Cells pre-treated with 10 µg/ml MAb-mTLR2 or DMSO and co-cultured with/without 5µg/ml Pam3SCK4. Representative images from at least three independent assays are shown. Scale bar 50 µm.

E. Bar graphs show increased proliferation of HFSC in the presents of TLR2 ligand Pam3SCK4 with no effect in MAb-mTLR2 pre-treated cells compared to control. N=6 independent experiments.

F. Dysregulated genes were confirmed by RNA sequencing or qPCR of FACS-sorted HFSCs from the first telogen dorsal skin of TLR2lox$^{/lox}$ and TLR2$^{HFSC-KO}$ mice. HFSCs from 4 mice in each group were sorted and sequenced. Dysregulated genes in RNA sequencing were those with an adjusted p-value < 0.05.

G. Dysregulated pathways in HFSCs lacking TLR2.

H. Representative confocal images of competent telogen follicles from WT or TLR2^{KO} mice immunostained for CD34 and pSmad1/5/9. Stars label hair shaft. Scale bars are 10 µm.

I. Quantification of pSmad1/5/9$^+$ bulge stem cell number in images from H shows significantly more pSmad1/5/9$^+$ cells in WT hair follicle bulge region compared with TLR2^{KO} hair follicles. N = 4 for each group.

J. Representative confocal images of TLR2$^{lox/lox}$ and TLR2$^{HFSC-KO}$ telogen hair follicles immunostained for β-catenin showed no difference between the two groups. Stars label the hair shaft. Scale bars are 20 µm.

All bar graphs are mean ± s.e.m. Non-parametric Mann-Whitney test (I), or Kruskal-Wallis test with Dunn's multiple comparisons test (C), or one-way ANOVA with Tukey's multiple comparisons test (E) was used to determine statistical differences. For the WB quantification with experiments with n=3, the minimum achievable p-value for the non-parametric tests is 0.1000.
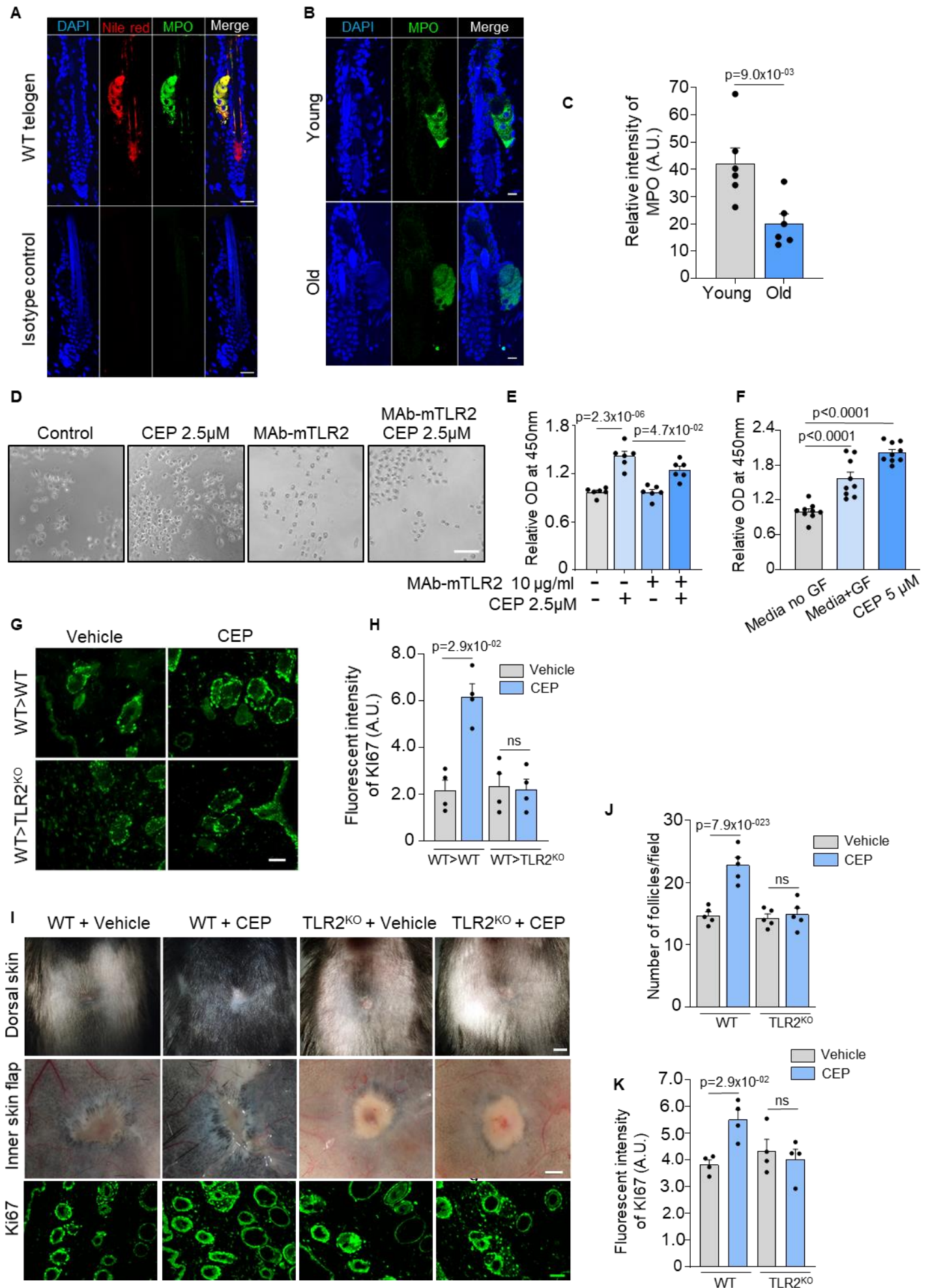
Supplementary figure 5

Fig. S5.

The promotion of hair follicle regeneration after wound healing is dependent on TLR2

A. Representative confocal images of Nile red-labeled (sebaceous gland) WT telogen hair follicles co-immunostained for myeloperoxidase (MPO) showing complete co-localization of MPO to the sebaceous gland. The isotype control panel shows the images of hair follicles stained with MPO isotype control antibody. Scale bars are 20 μm.

B. Representative confocal images of hair follicles from old vs young mice stained for MPO. Scale bars are 10 μm.

C. Quantification of MPO fluorescent intensity in B showing significantly less MPO in hair follicles from older mice. N = 6 for each group.

D. Representative microphotographs of Human Hair Follicle Stem Cells pre-treated with 10 μg/ml MAb-mTLR2 or DMSO and co-cultured with/without 2.5μM of CEP. Representative images from at least three independent assays are shown. Scale bar 50 μm.

E. Bar graphs show increased proliferation of HFSC in the presence of TLR2 endogenous ligand CEP compared to control, which was abolished in the presence of TLR2 blocking antibody. N=6 independent experiments.

F. Bar graphs show increased proliferation of Human Hair Follicle Dermal Papilla Cells incubated with 5μM of CEP compared to the control. N=9 independent experiments.

G. Representative confocal images of Ki67 immunostaining of dorsal skin adjacent to wound of CEP-treated WT bone-marrow transplanted WT and TLR2^{KO} mice. Scale bars are 50 μm.

H. Quantitative results showed increased Ki67 intensity in hair follicles around wounds of CEP-treated WT bone-marrow transplanted WT mice with no differences in TLR2^{KO} with WT bone marrow. N = 4 per group.

I. Representative photographs of dorsal skin (upper panels), inner skin flaps (middle panels), and representative confocal images of Ki67 immunostaining (lower panels) of vehicle- or CEP-treated WT or TLR2^{KO} skin. Scale bars are 1 mm for dorsal skin, 500 μm for skin flaps, and 50 μm for confocal images.

J. Bar graph showing quantification of hair follicle numbers of vehicle or CEP-treated skin from I. N = 5 per group.

K. Bar graph showing quantification of Ki67 fluorescent intensity of Ki67 staining of vehicle or CEP-treated skin from I. N = 4 per group.

Unpaired two-tailed t-test (C), or non-parametric Mann-Whitney test (H, J, K), or Kruskal-Wallis test with Dunn's multiple comparisons test (F), or one-way ANOVA with Tukey's multiple comparisons test (E) was used to determine statistical differences. All bar graphs are mean ± s.e.m.

Table S1.

Target	Primers
Bmp7	ACGGACAGGGCTTCTCCTAC
Bmp7	ATGGTGGTATCGAGGGTGGAA
Bmp2	GGGACCCGCTGTCTTCTAGT
Bmp2	TCAACTCAAATTCGCTGAGGAC
Bmpr1a	AACAGCGATGAATGTCTTCGAG
Bmpr1a	GTCTGGAGGCTGGATTATGGG
Nfkb2	GGCCGGAAGACCTATCCTACT
Nfkb2	CTACAGACACAGCGCACACT
IL1b	GCAACTGTTCCTGAACTCAACT
IL1b	ATCTTTTGGGGTCCGTCAACT
IL6	TAGTCCTTCCTACCCCAATTTCC
IL6	TTGGTCCTTAGCCACTCCTTC
Hey1	GCGCGGACGAGAATGGAAA
Hey1	TCAGGTGATCCACAGTCATCTG
Notch1	ACACTGACCAACAAATGGAGG
Notch1	GTGCTGAGGCAAGGATTGGA
Hes1	CCAGCCAGTGTCAACACGA
Hes1	AATGCCGGGAGCTATCTTTCT
Bcl2a1a	GGCTGAGCACTACCTTCAGTA
Bcl2a1a	TGGCGGTATCTATGGATTCCAC
Myc	ATGCCCCTCAACGTGAACTTC
Myc	CGCAACATAGGATGGAGAGCA
Tlr2	TCTAAAGTCGATCCGCGACAT
Tlr2	CTACGGGCAGTGGTGAAAACT

qPCR primers.